

A redox-activated theranostic nanoplatform: toward glutathione-response imaging guided enhanced-photodynamic therapy

Xiaochun Hu^{#a}, Zhenli Xu^{#a}, Jiwen Hu^c, Chunyan Dong^b, Yonglin Lu^b, Xuewen Wu^a, Maierhaba Wumaier^a, Tianming Yao^{*a}, Shuo Shi^{*a,b}

Contribute equally to this work

a. Shanghai Key Lab of Chemical Assessment and Sustainability, School of Chemical Science and Engineering, Tongji University, 1239 Siping Road, 200092 Shanghai, P.R. China.

b. Breast Cancer Center, Shanghai East Hospital, Tongji University, 200120 Shanghai, P.R. China.

c. School of Environmental and Chemical Engineering, Shanghai University, Shanghai, 200444, P.R. China

E-mail: shishuo@tongji.edu.cn, tmyao@tongji.edu.cn

Table of contents

| | |
|--|------|
| Figure S1. Synthetic route for RA | S-2 |
| Figure S2. ¹ H NMR spectrum of RA | S-3 |
| Figure S3. ¹³ C NMR spectrum of RA | S-4 |
| Figure S4. TOF-MS for RA | S-5 |
| Figure S5. The rate of system to generate ¹ O ₂ | S-5 |
| Figure S6. The ¹ O ₂ quantum yield of RA | S-6 |
| Figure S7. The geometric structure of RA, HOMO–LUMO distribution of RA and the energy of first excited triplet state (T1) | S-6 |
| Figure S8. UV-vis absorption spectra of DCNPs-C and DCMn | S-7 |
| Figure S9. Elemental analysis of the DCMn by Electron diffraction spectroscopy (EDS) spectrum | S-7 |
| Figure S10. The XPS high-resolution scans of Mn 2p peaks | S-7 |
| Figure S11. Photoluminescence spectrum of NPs following excitation with an 808 nm laser | S-8 |
| Figure S12. Zeta-potential of DCMn and DCMn-RA | S-8 |
| Figure S13. Relationship between longitudinal or transverse rates of DCMn-RA and the different GSH concentrations | S-9 |
| Figure S14. Emission spectra of DCFH incubated with two photosensitizers in presence or absence of 10 mM GSH after 1 min irradiation | S-9 |
| Figure S15. Mean fluorescence intensity of cells and intracellular GSH detections of MDA-MB-231 cells | S-9 |
| Figure S16. Confocal images of MDA-MB-231 cells incubated with DCMn-RA | S-10 |
| Figure S17. Cytotoxicity of free RA for MDA-MB-231 cells | S-10 |
| References | S-10 |

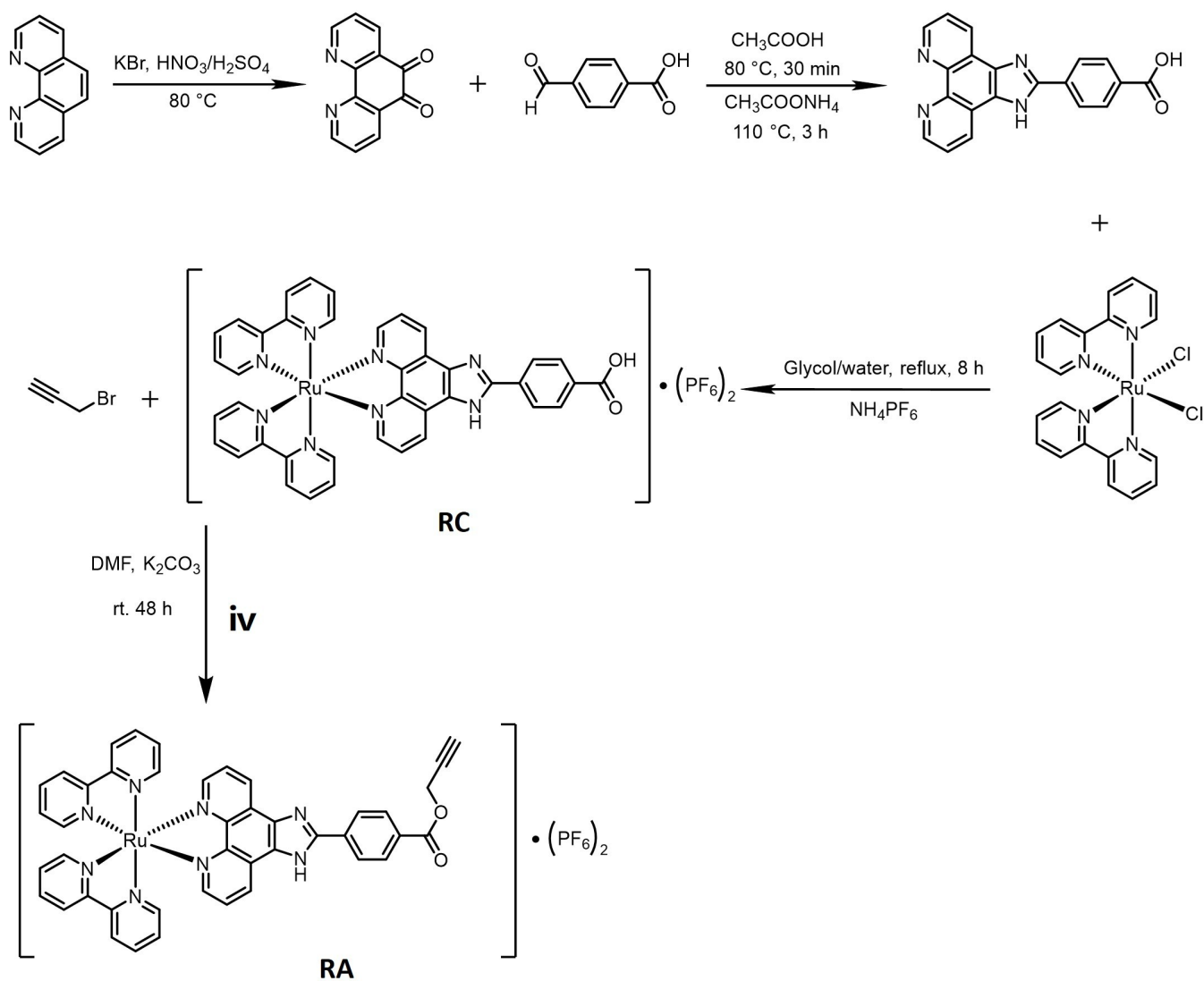


Figure S1. Synthetic route for RA. The details for **iv**: RC (0.38 mmol) and K_2CO_3 (0.38 mmol) were suspended in DMF (3 mL). Propargyl bromide (1.14 mmol) was added and the reaction mixture was stirred at room temperature for 48 h under argon. Upon addition of 10 mL water, the precipitated complex was washed with water (4×30 mL), and purified by chromatography over alumina by using MeCN as eluent.

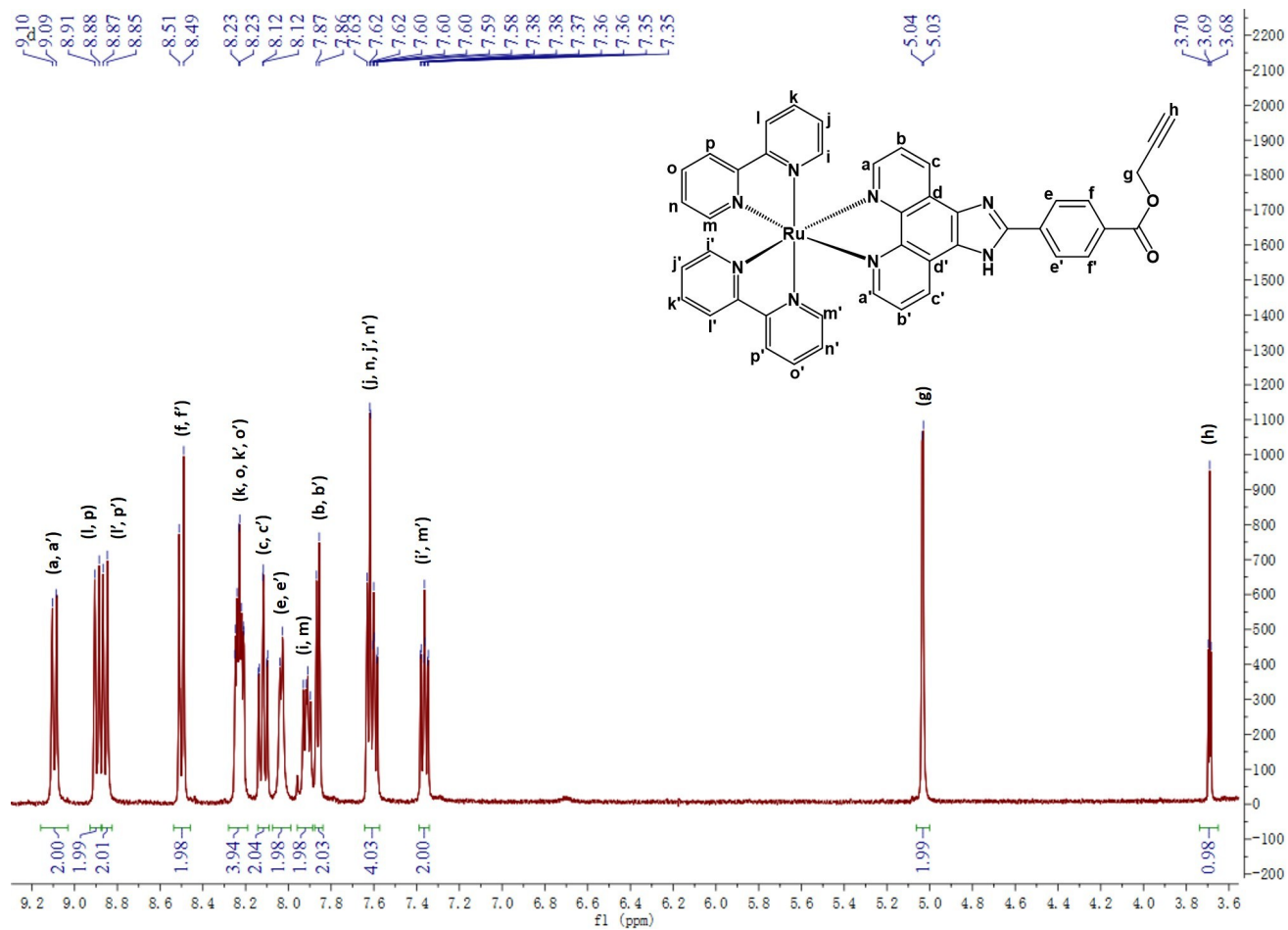


Figure S2. ¹H NMR spectrum of RA. ¹H NMR (400 MHz, DMSO) δ 9.09 (d, J = 7.5 Hz, 2H), 8.90 (d, J = 8.4 Hz, 2H), 8.86 (d, J = 8.2 Hz, 2H), 8.50 (d, J = 8.6 Hz, 2H), 8.23 (ddd, J = 8.0, 4.4, 1.4 Hz, 4H), 8.12 (td, J = 8.0, 1.4 Hz, 2H), 8.03 (d, J = 4.7 Hz, 2H), 7.91 (dd, J = 8.2, 5.3 Hz, 2H), 7.86 (d, J = 4.9 Hz, 2H), 7.60 (ddd, J = 7.2, 5.8, 3.1 Hz, 4H), 7.39 – 7.34 (m, 2H), 5.03 (d, J = 2.4 Hz, 2H), 3.69 (t, J = 2.4 Hz, 1H).

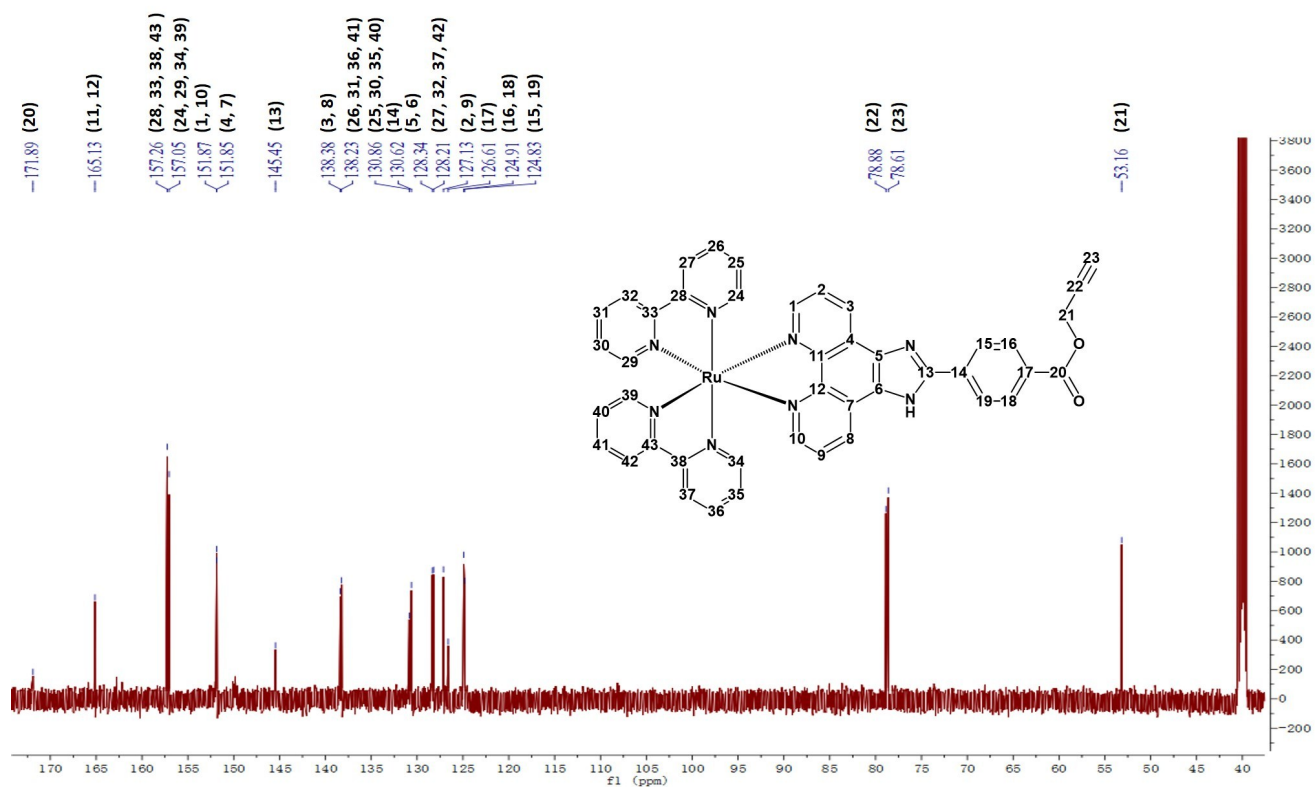


Figure S3. ^{13}C NMR spectrum of RA. ^{13}C NMR (151 MHz, DMSO) δ 171.89, 165.13, 157.26, 157.05, 151.87, 151.85, 145.45, 138.38, 138.23, 130.86, 130.62, 128.34, 128.21, 127.13, 126.61, 124.91, 124.83, 78.88, 78.61, 53.16.

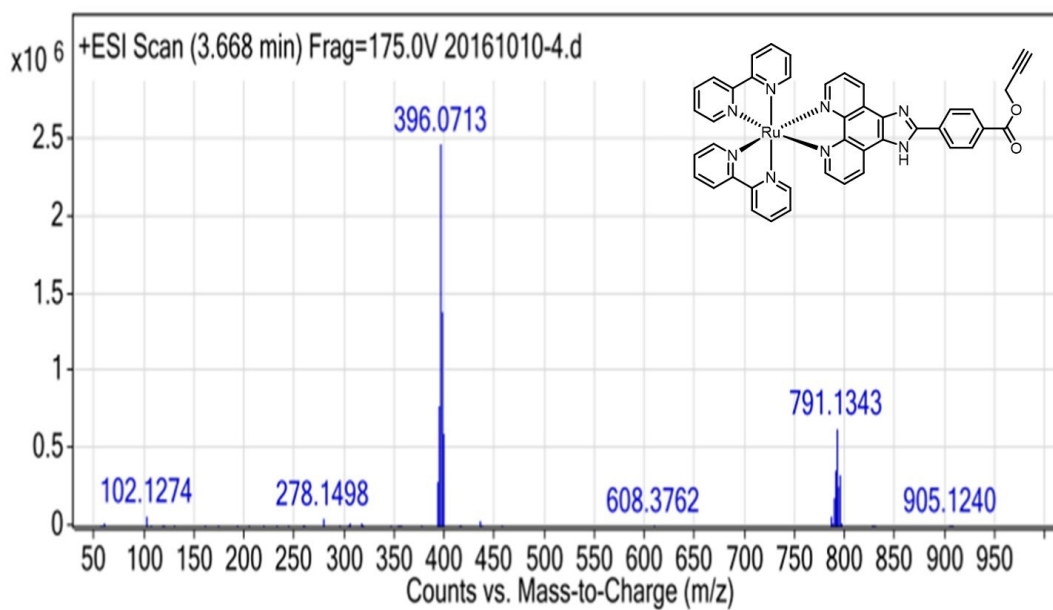


Figure S4. TOF-MS for $[\text{C}_{43}\text{H}_{30}\text{N}_8\text{O}_2\text{Ru}]^{2+}$: Calc. 792.15, found m/z 396.0713 ($\text{M}^{2+}/2$).

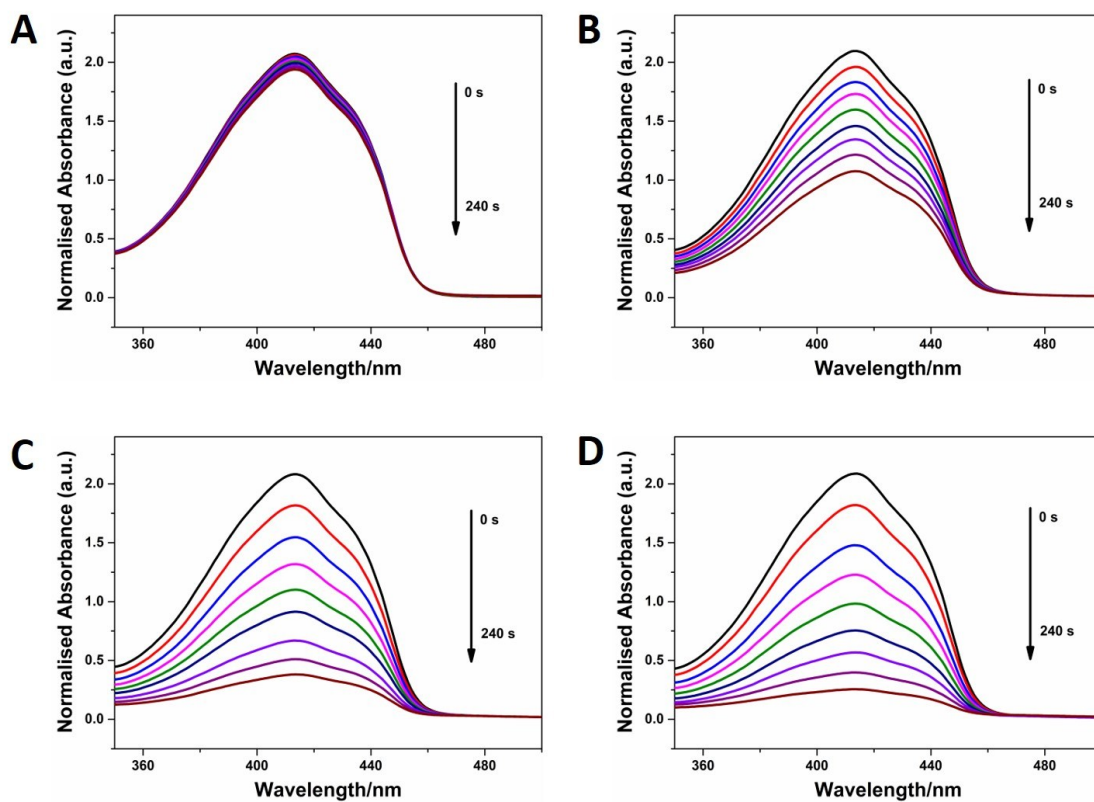


Figure S5. 1,3-diphenylisobenzofuran (DPBF) was used as trap to monitor the rate of system to generate $^1\text{O}_2$, and the absorption spectra DPBF was recorded at 30 s intervals. The rate of singlet oxygen generation was determined from the decrease absorption intensity at 414 nm over time. (A) Time-dependent absorption spectra of DPBF (in DMF, 10 μM) interval 30 s upon irradiation at 450 nm. Time dependent absorption spectra of DPBF (in DMF, 10 μM) upon irradiation at 450 nm in the presence of 2 μM (B) $[\text{Ru}(\text{bpy})_3]^{2+}$, (C) RC and (D) RA.

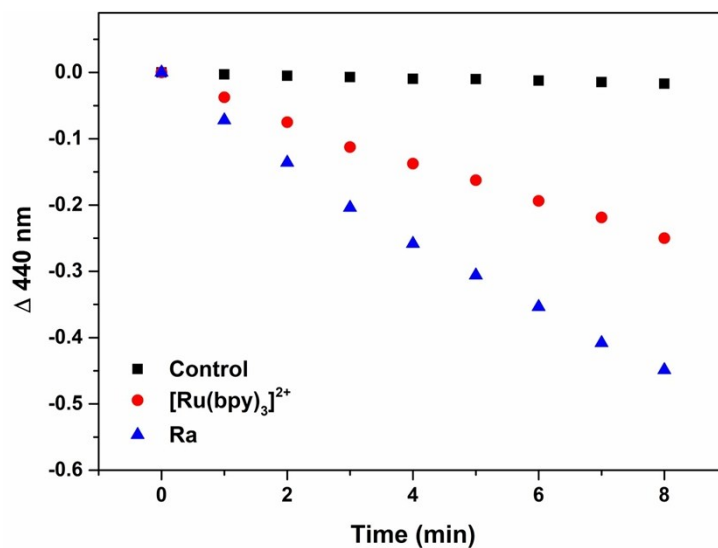


Figure S6. In the absence or presence of RA (10 μM), changes in the absorption spectra of *p*-nitrosodimethylaniline (RNO) (25 μM) at 440 nm upon 450 nm irradiation in aerated PBS were measured. $[\text{Ru}(\text{bpy})_3]^{2+}$ was used as the standard, the $^1\text{O}_2$ quantum yield of $[\text{Ru}(\text{bpy})_3]^{2+}$ is 0.18 in H_2O .¹

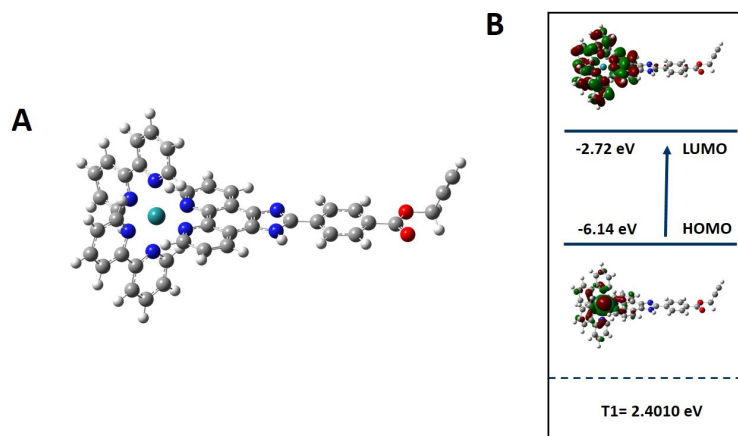


Figure S7. (A) The geometric structure of RA. (B) HOMO–LUMO distribution of RA and the energy of first excited triplet state (T1) of RA (B3LYP/SDD/6-311G** by Gaussian 09).^{2,3}

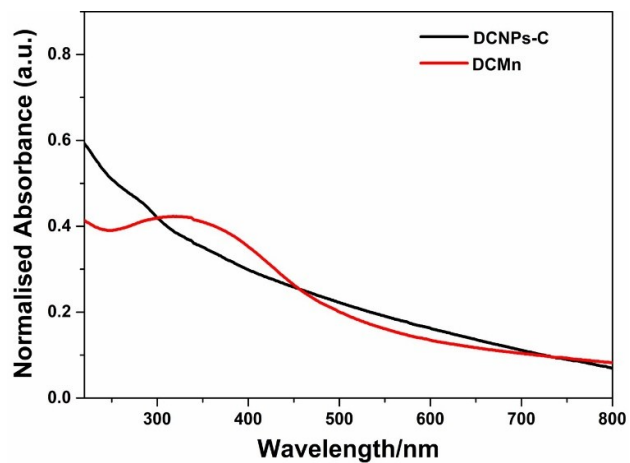


Figure S8. UV-vis absorption spectra of DCNPs-C and DCMn.

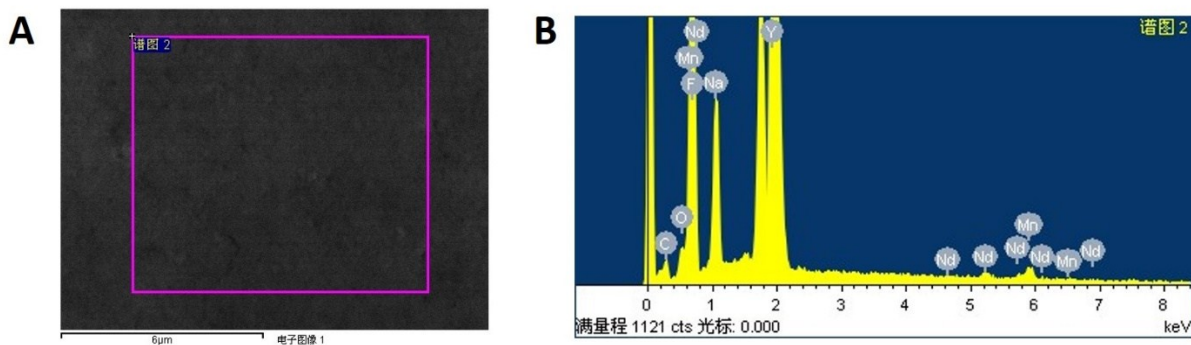


Figure S9. Elemental analysis of the DCMn by Electron diffraction spectroscopy (EDS) spectrum.

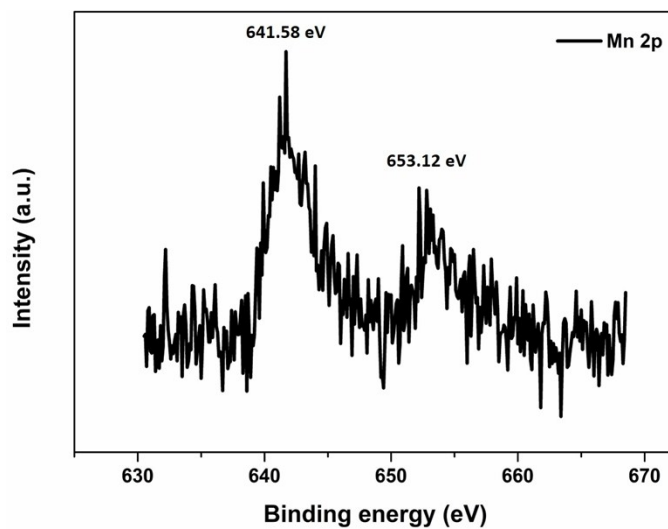


Figure S10. The XPS high-resolution scans of Mn 2p peaks.

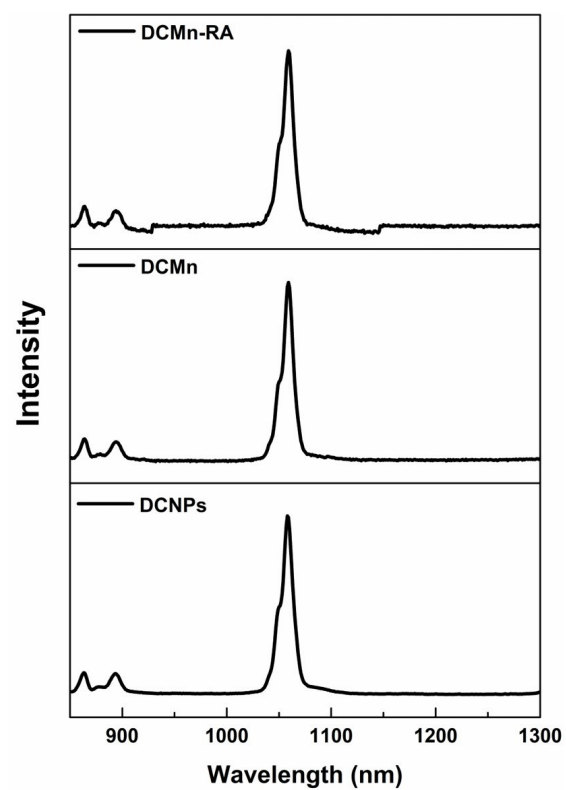


Figure S11. Photoluminescence spectrum of NPs following excitation with an 808 nm laser (0.6 W/cm^2).

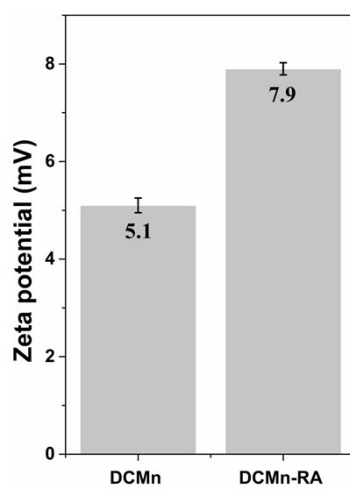


Figure S12. Zeta-potential of DCMn and DCMn-RA.

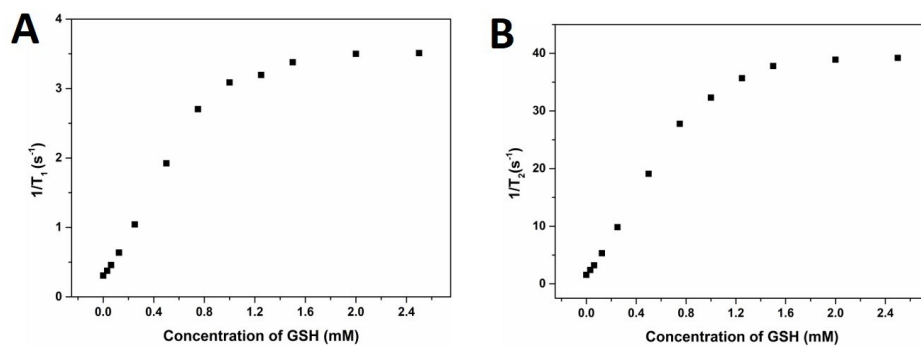


Figure S13. Relationship between (A) longitudinal or (B) transverse rates of DCMn-RA and the different GSH concentrations.

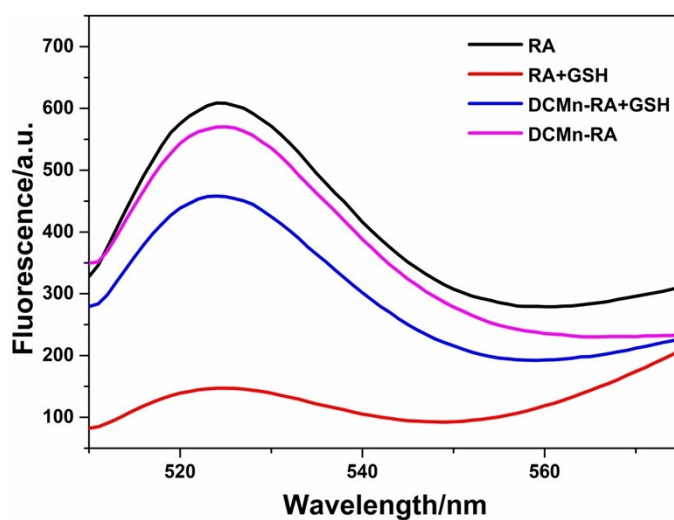


Figure S14. Emission spectra of DCFH incubated with two photosensitizers in presence or absence of 10 mM GSH after 1 min irradiation (450 nm, 15 mW/cm²).

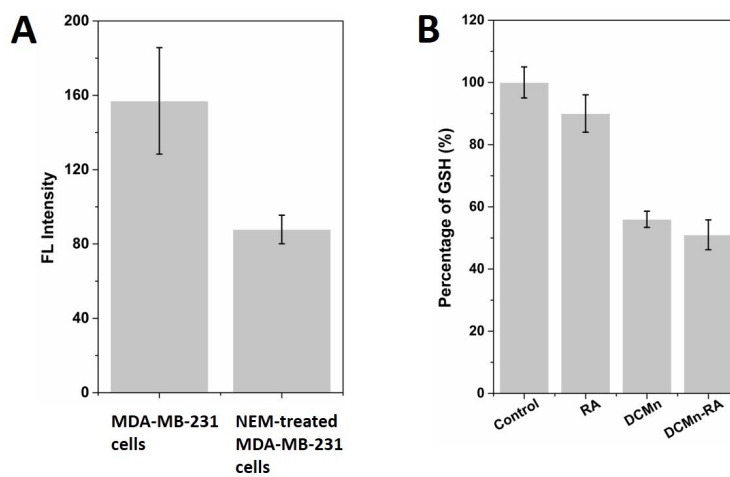


Figure S15. (A) Mean fluorescence intensity of cells for Figure 5(A) and Figure 5(B), respectively. (B) Intracellular GSH detections of MDA-MB-231 cells after various treatments, including blank group as a control, free RA, DCMn and DCMn-RA.



Figure S16. Confocal images of MDA-MB-231 cells incubated with DCMn-RA. Red channel image was obtained from DCMn-RA. The blue channel image was obtained from Hoechst (nucleus). Scale bars =20 μm .

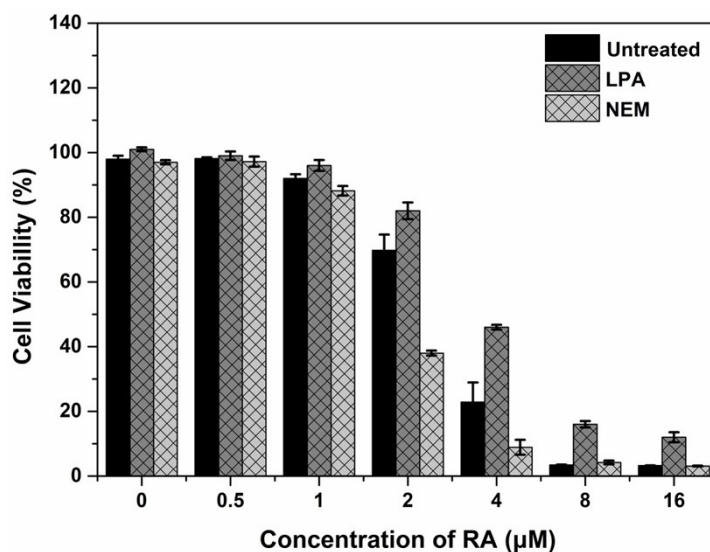


Figure S17. Cytotoxicity of free RA for MDA-MB-231 cells treated with LPA (a GSH synthesis enhancer, 0.5 mM) or NEM (a GSH scavenger, 0.5 mM) before irradiation.

1. D. Zhang, Y. Zheng, C. Tan, J. Sun, W. Zhang, L. Ji and Z. Mao, *ACS Appl. Mater. Inter.*, 2017, **9**, 6761-6771.
2. X. Hu, D. Yang, T. Yao, R. Gao, M. Wumaier and S. Shi, *Dalton Trans.*, 2018, **47**, 5422-5430.
3. S. Shi, X. Gao, H. Huang, J. Zhao and T. Yao, *Chem. Eur. J.*, 2015, **21**, 13390-13400.